Quantification of nucleolar channel systems: uniform presence throughout the upper endometrial cavity

Michael J. Szmyga, M.S.,[a] Eli A. Rybak, M.D., M.P.H.,[a,b,e] Edward J. Nejat, M.D., M.B.A.,[a,b] Erika H. Banks, M.D.,[b] Kathleen D. Whitney, M.D.,[c] Alex J. Polotsky, M.D., M.S.,[b] Debra S. Heller, M.D.,[d] and U. Thomas Meier, Ph.D.[a]

[a] Department of Anatomy and Structural Biology, [b] Department of Obstetrics & Gynecology and Women's Health, and [c] Department of Pathology, Albert Einstein College of Medicine, Bronx, New York; [d] Department of Pathology, University of Medicine and Dentistry of New Jersey–New Jersey Medical School, Newark, New Jersey; and [e] currently Reproductive Medicine Associates of New Jersey, Morristown, New Jersey

Objective: To determine the prevalence of nucleolar channel systems (NCSs) by uterine region, applying continuous quantification.
Design: Prospective clinical study.
Setting: Tertiary care academic medical center.
Patient(s): Forty-two naturally cycling women who underwent hysterectomy for benign indications.
Intervention(s): NCS presence was quantified by a novel method in six uterine regions—fundus, left cornu, right cornu, anterior body, posterior body, and lower uterine segment (LUS)—with the use of indirect immunofluorescence.
Main Outcome Measure(s): Percentage of endometrial epithelial cells (EECs) with NCSs per uterine region.
Result(s): NCS quantification was observer independent (intraclass correlation coefficient 0.96) and its intrasample variability low (coefficient of variation 0.06). Eleven of 42 hysterectomy specimens were midluteal, ten of which were analyzable with nine containing >5% EECs with NCSs in at least one region. The percentage of EECs with NCSs varied significantly between the LUS (6.1%; interquartile range [IQR] 3.0–9.9) and the upper five regions (16.9%; IQR 12.7–23.4), with fewer NCSs in the basal layer of the endometrium (17 ± 6%) versus the middle (46 ± 9%) and luminal layers (38 ± 9%) of all six regions.
Conclusion(s): NCS quantification during the midluteal phase demonstrates uniform presence throughout the endometrial cavity, excluding the LUS, with a preference for the functional luminal layers. Our quantitative NCS evaluation provides a benchmark for future studies and further supports NCS presence as a potential marker for the window of implantation.
(Fertil Steril® 2013;99:558–64. ©2013 by American Society for Reproductive Medicine.)
Key Words: Nucleolar channel system (NCS), endometrium, receptivity, secretory transformation

Discuss: You can discuss this article with its authors and with other ASRM members at http://fertstertforum.com/szmygamj-nucleolar-channel-system-endometrium/

Use your smartphone to scan this QR code and connect to the discussion forum for this article now.*

* Download a free QR code scanner by searching for "QR scanner" in your smartphone's app store or app marketplace.

Received June 25, 2012; revised October 3, 2012; accepted October 12, 2012; published online November 6, 2012.
M.J.S. has nothing to disclose. E.A.R. has nothing to disclose. E.J.N. has nothing to disclose. E.H.B. has nothing to disclose. K.D.W. has nothing to disclose. A.J.P. has an unrestricted research grant from Bayer (unrelated to the submitted work). D.S.H. has been reimbursed for travel to speak at meetings for the College of American Pathologists and International Society for the Study of Vulvar Disease, receives minimal book royalties, and provides occasional medicolegal expert testimony (all unrelated to the submitted work). U.T.M. has nothing to disclose.
M.J.S. and E.A.R. contributed equally to this work.
A.J.P.'s current affiliation is Department of Obstetrics and Gynecology, University of Colorado, Denver, Colorado.
Supported by the March of Dimes Birth Defects Foundation (no. 1-FY09-363 to U.T.M.) and CMBG Training Program (T32 GM007491 to M.J.S.).
Reprint requests: U. Thomas Meier, Ph.D., Department of Anatomy and Structural Biology, Albert Einstein College of Medicine, 1300 Morris Park Avenue, Bronx, New York 10461 (E-mail: tom.meier@einstein.yu.edu).

Fertility and Sterility® Vol. 99, No. 2, February 2013 0015-0282/$36.00

http://dx.doi.org/10.1016/j.fertnstert.2012.10.027

The nucleolar channel system (NCS) is an enigmatic structure associated with secretory transformation of the endometrium (1). Discovered on the ultrastructural level a half-century ago (2), the NCS is a membranous organelle of uniform size, ~1 μm in diameter, that develops transiently in the nuclei of secretory phase endometrial epithelial cells (EECs) (3–5). In previous work, we established a light microscopic method to stain and identify NCSs via an immunofluorescence approach

using an antibody directed against a subset of nuclear pore complex proteins, which are major components of the NCS (6). We determined that NCSs are present in roughly one-half of all EEC nuclei during a period overlapping with the implantation window: cycle days (CDs) 19–24 of an idealized 28-day cycle. The NCS is specific to healthy human EECs; it is not detected in endometrial stromal cell nuclei, human breast, or gastrointestinal tract tissue, endometrial carcinoma specimens, or in baboon endometrium (6). Moreover, midluteal NCS presence is robust and independent from fertility status, including unexplained infertility (7–9).

Given this robust midluteal appearance of NCSs, their sensitivity to progesterone, and their absence in pregnancy, among other evidence, we suggest that they play a role in endometrial receptivity (5, 10–15). Although the literature is sparse regarding possible regional disparities in endometrial receptivity, it is interesting to note that ultrastructural evidence indicates localized concentrations of NCSs (16). The preferred location within the endometrial cavity for blastocyst implantation in both spontaneous and assisted conception, however, is neither clearly known nor well studied. Table 1 lists several reports that have investigated the endometrial region–specific implantation frequency of blastocysts via anatomic dissection or ultrasonography (17–20). These studies collectively suggest that the cornual region might prove to be most favorable for blastocyst implantation. Accordingly, we hypothesized that NCS presence varies by uterine region and sought to determine the regional prevalence of NCSs within the endometrial cavity. To fully appreciate NCS prevalence and to provide a benchmark for future studies, we developed an absolute NCS quantification method based on our semiquantitative light microscopic detection method (6).

MATERIALS AND METHODS

Specimens

Uterine specimens were obtained from patients who underwent hysterectomy for benign gynecologic indications (predominantly menorrhagia attributed to uterine fibroids) at Montefiore Medical Center, a tertiary-care academic medical center in The Bronx, New York, affiliated with the Albert Einstein College of Medicine, from November 2008 through August 2009. Institutional Review Board approval was obtained for this study. Specific patient data were deidentified. Clinical information provided for each specimen was limited to a deidentified final pathology report and to data transcribed by the operating team on a "study sheet" that was distributed by the operating room nursing staff before every hysterectomy case, and which accompanied the specimen from the operating room to the surgical pathology department. Enrollment criteria were established in an effort to enroll all women who were postovulatory (based on self-reported last menstrual period [LMP]). Exclusion criteria fell under three categories. First, any case with known or suspected malignancy or endometrial hyperplasia was excluded. Logistically, such cases warranted more extensive endometrial sampling and longer-term preservation of the hysterectomy specimens for clinical purposes. Moreover, NCS presence has not been detected in cases of

TABLE 1

Studies investigating the region-specific implantation frequency of blastocysts within the endometrial cavity.

	Hertig 1956 (20)	Kawakami 1993 (18)	Minami 2003 (19)	Cavagna 2006 (17)
Design	Anatomic dissection of 211 hysterectomy specimens derived from women of known fertility, a subset of which were derived from women during the luteal phase with early pregnancies, some having already implanted	Two-dimensional transvaginal ultrasonography on fertility clinic patients during the follicular phase and before 6 weeks' gestation dated by basal body temperature	Three-dimensional transvaginal ultrasonography on unselected women with gestational sacs measuring 3–6 mm	Three-dimensional transvaginal ultrasonography performed 21–24 days after embryo transfer (ET) on women with singleton pregnancies having undergone intracytoplasmic sperm injection and ultrasound-guided ET intentionally directed to the midpoint between the internal os and fundus
Sample size	26	21	138	47
Conception	Spontaneous	Spontaneous	Spontaneous	Assisted
Fundus (midline)	100% in upper cavity: 58% ipsilateral to corpus luteum, 4% midline, 38% contralateral to corpus luteum	Upper versus middle cavity not specified: 81% ipsilateral to dominant follicle, 14% midline, 5% contralateral to dominant follicle	16% 39% 34%	34% 15% 17%
Left cornu				
Right cornu				
Anterior body			9% middle cavity region	30% middle cavity region
Posterior body				
Lower uterine segment			2%	4%

Szmyga. NCSs appear throughout the endometrium. Fertil Steril 2013.

endometrial adenocarcinoma (6). Second, any case involving morcellation of the uterus (i.e., laparoscopic supracervical hysterectomy) was excluded, given the obvious inability to identify specific uterine regions. Finally, any specimen deemed unlikely to demonstrate secretory-phase endometrium was excluded at the outset. Specifically, if the patient's self-reported LMP, as recorded in the preoperative nurse interview, was <10 days before surgery, or if the patient was exposed to GnRH agonist (e.g., leuprolide) or to any estrogen and/or progestin therapy during the 3-month preoperative period, or if the patient was aged ≥ 50 years, then the appropriate checkboxes on the study sheet would trigger exclusion of the specimen from the study.

Background Information

The following information was obtained by the surgical team after reviewing the preoperative history form in the patient's chart, and then entered onto the study sheet: age, parity, self-reported LMP, obstetrical and gynecologic surgical history, and indication for hysterectomy. Additionally, the type of hysterectomy performed (abdominal vs. vaginal vs. laparoscopic; total vs. supracervical) was recorded. In addition to diagnosing and describing any pathology, the final pathology report detailed the uterine weight and the presence and location (intramural vs. submucosal vs. subserosal) of any fibroids. Of note, the pathologist labeled each endometrium as secretory, proliferative, or inactive. Slides from uteri determined to be secretory were subsequently provided to another pathologist (D.S.H.) with specific expertise in classical histologic dating with the use of Noyes criteria (21), given the obvious limitations with relying solely on the self-reported LMP. Recognizing, however, the substantial intersubject, intrasubject, and interobserver variability that limit the precision of histologic dating with the use of Noyes criteria (22), we limited our use of histologic dating to merely identify the specimens that demonstrated a histologic date within CDs 18–24 and were thereby deemed to be midluteal.

Processing and Immunostaining of Tissue Sections

Upon removal from the pelvis, uterine specimens were transported immediately for sectioning by the surgical pathology staff. If the uteri could not be sectioned within 15 minutes, before placing them in 10% formalin, they were sliced coronally through the endometrium to minimize endometrial autolysis that could adversely affect subsequent immunostaining (23, 24). Sections of endometrium were obtained from six different regions of the endometrial cavity: fundus, left cornu, right cornu, anterior body, posterior body, and lower uterine segment (LUS). The tissue samples were then paraffin embedded, sectioned, and mounted on slides.

Immunostaining was performed as previously described (6, 7). Briefly, tissue sections were deparaffinized, rehydrated, and (for antigen retrieval) treated with 10 mmol/L sodium citrate (pH 6.0). The slides were then immersed in -20°C methanol for 5 minutes to optimize immunostaining. After complete air drying, the slides were rehydrated with phosphate-buffered saline solution. NCSs were detected by indirect immunofluorescence with the use of the monoclonal antibody 414 (mAb414; Covance) and DyLight488-labeled secondary antibodies (Jackson Immunoresearch) as previously described (6). Nuclei were detected by staining with 4′,6-diamidino-2-phenylindole (DAPI) at 1 μg/mL. For preservation, samples were postfixed with 4% paraformaldehyde. All tissue samples were analyzed for the presence of NCSs by two independent observers as described previously (7) and the samples from the uteri with $>5\%$ EECs with NCSs in at least one region were fully quantified by the newly developed method described below.

Imaging and Quantification of NCSs

All samples were imaged on a DeltaVision Core system (Applied Precision) with an Olympus IX71 stand using a $\times 60$/1.42 NA Planapo objective and a Photometrics CoolSnap HQ2 CCD camera. To be blinded regarding NCS presence, ten areas/fields with endometrial glands of each paraffin section were randomly selected based on nuclear DNA staining using the DAPI channel. Subsequently, Z-series of optical planes across the entire paraffin section were collected in 0.3-μm steps in both channels, DAPI (to count nuclei, i.e., EECs) and fluorescein isothiocyanate (to count NCSs). For deconvolution, softWoRx 3.6.0 (Applied Precision) was used with the enhanced ratio method, medium filter, and ten iterations. Deconvolved Z-series were viewed in ImageJ (National Institutes of Health). Staining of nuclear pore complexes by mAb414 served as internal control for the staining procedure, and sections were analyzed only if the pores could be clearly distinguished (Fig. 1A). NCSs and EEC nuclei were analyzed manually with the use of the ImageJ multipoint tool to mark and count each NCS and nucleus. Nuclei were counted in a maximum projection of all planes of one area/field. NCSs were counted in each individual plane, viewed as image series to verify in adjacent planes that the signal was gradually lost thereby identifying the structures as the 1-μm-diameter NCSs not only within the plane but in all dimensions (Fig. 1A). The number of NCSs in ten random areas/fields was summed and divided by the number of EEC nuclei to obtain the percentage of EECs with NCSs for each specimen. In this manner, from 459 to 1,182 EECs (765 ± 154) were counted for each of the 53 samples (one section had insufficient epithelial tissue for analysis). A total of 40,565 nuclei and 7,471 NCSs were counted.

The method was validated on a set of images of 24 endometrial biopsies with NCSs and one without. Specifically, two independent observers counted an average of 15,473 nuclei and 928 NCSs. To assess intrasample variability, 15 consecutive 7-μm-thick paraffin sections were prepared and five randomly selected sections (nos. 1, 6, 9, 12, and 14) analyzed for percentage of EECs with NCSs. A total of 3,959 nuclei and 907 NCSs were counted.

To assess the local distribution of NCSs throughout the different layers of the endometrium, paraffin sections from all six regions of a single uterus were hematoxylin and eosin (H&E)–stained and the images of the individual regions stitched together with the use of Adobe Photoshop CS5. The imaged epithelium was evenly divided into three layers (basal, middle, and luminal) and the number of glands for each layer

FIGURE 1

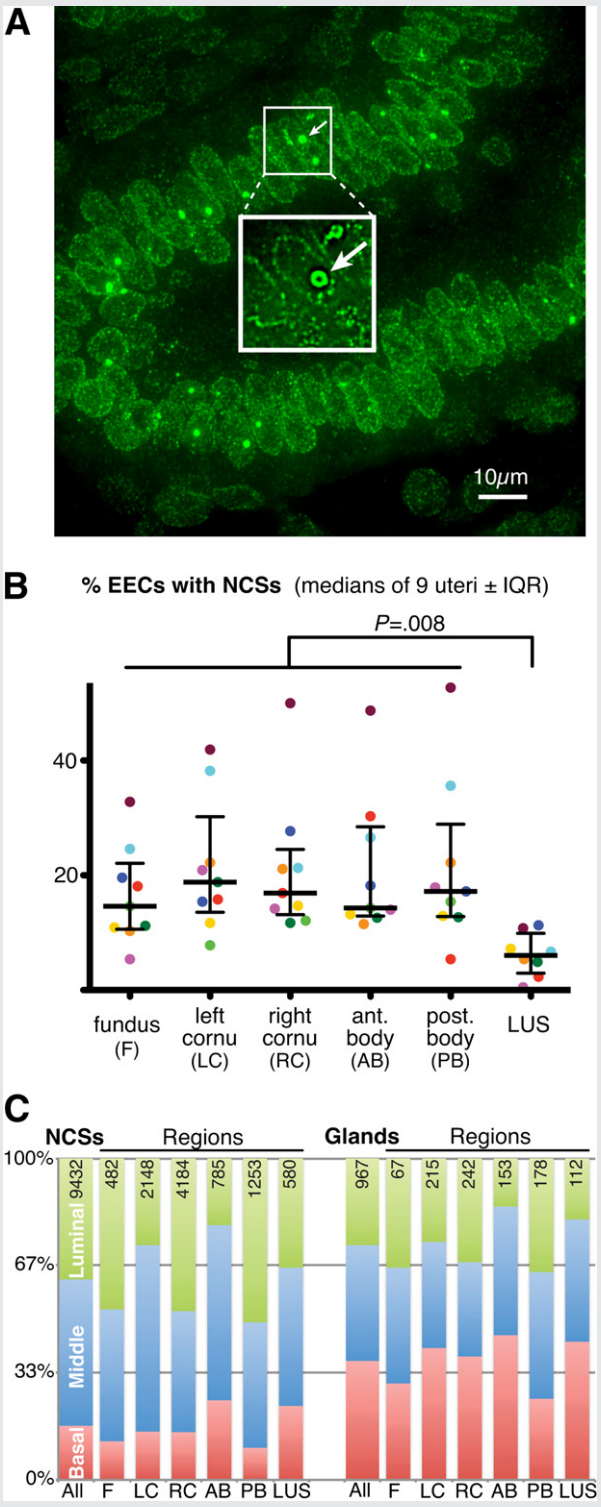

(A) Endometrial gland: indirect immunofluorescence of nuclear pore complex proteins that are highly enriched in nucleolar channel systems (NCSs; one is indicated by an *arrow*) on one of the ten random optical fields analyzed for the anterior body region of one uterus (*red* in B). A maximum projection of 22 0.3-μm-thick optical sections is shown. Inset: twofold magnification of a single optical section from the *boxed area* above; note that in that optical plane only two of the three NCSs seen in the maximum projection are visible (i.e., the NCS in the lower right corner is situated on a different plane), and note the outline of the nuclear boundary by the individual pore complexes. (B) Regional prevalence of NCSs in the uterus. Percentage of endometrial epithelial cells (EECs) with NCSs in six regions of nine uteri (colors indicate patients as numbered in Table 2: *blue* = 1; *light green* = 2; *purple* = 3; *light blue* = 4; *orange* = 5; *red* = 6; *brown* = 7; *green* = 8; *yellow* = 9). The median ± interquartile range (IQR) is indicated for each region, as is the significant difference between the lower uterine segment (LUS) and the other five regions (P=.008; Wilcoxon signed ranks test). (C) Prevalence of NCSs in the endometrial layers. The distribution of NCSs (left) and glands (right) between three equal layers (basal, middle, and luminal) of the endometrium of one uterus (*yellow* in B) is indicated for all regions together (first column each) and for each individual region. The numbers correspond to 100% of each column. Note the reduced amount of NCSs in the basal layer compared with the middle and luminal ones. F = fundus; LC = left cornu; RC = right cornu; AB = anterior body; PB = posterior body.

Szmyga. NCSs appear throughout the endometrium. Fertil Steril 2013.

FIGURE 1 Continued

only two of the three NCSs seen in the maximum projection are visible (i.e., the NCS in the lower right corner is situated on a different plane), and note the outline of the nuclear boundary by the individual pore complexes. (B) Regional prevalence of NCSs in the uterus. Percentage of endometrial epithelial cells (EECs) with NCSs in six regions of nine uteri (colors indicate patients as numbered in Table 2: *blue* = 1; *light green* = 2; *purple* = 3; *light blue* = 4; *orange* = 5; *red* = 6; *brown* = 7; *green* = 8; *yellow* = 9). The median ± interquartile range (IQR) is indicated for each region, as is the significant difference between the lower uterine segment (LUS) and the other five regions (P=.008; Wilcoxon signed ranks test). (C) Prevalence of NCSs in the endometrial layers. The distribution of NCSs (left) and glands (right) between three equal layers (basal, middle, and luminal) of the endometrium of one uterus (*yellow* in B) is indicated for all regions together (first column each) and for each individual region. The numbers correspond to 100% of each column. Note the reduced amount of NCSs in the basal layer compared with the middle and luminal ones. F = fundus; LC = left cornu; RC = right cornu; AB = anterior body; PB = posterior body.

Szmyga. NCSs appear throughout the endometrium. Fertil Steril 2013.

determined. The number of NCSs in each layer was counted in immunostained paraffin sections that were successive to the H&E stained sections.

Outcome Measures and Statistical Analyses

To evaluate interobserver variability, we calculated the intraclass correlation coefficient (ICC) for the number of EECs and NCSs counted by two independent observers in 25 luteal endometrial biopsies with the use of Stata 11.0 (Stata Corp.). Additionally the correlation coefficient for the percentage of EECs with NCSs obtained between the two observers was calculated.

We tested our hypothesis that NCSs manifest a differential appearance pattern by uterine region. Our outcome of interest was the average percentage of EECs with NCSs for each uterine region. To determine the distribution of our data, a Shapiro-Wilk normality test was performed with the use of Prism 5 (GraphPad Software). Owing to the lack of normal distribution in two regions, a one-way analysis of variance (ANOVA; Friedman test) for nonparametric paired data was applied (P=.008) followed by a Wilcoxon signed ranks test for post hoc analysis. Friedman and Wilcoxon tests were performed with the use of R: A Language and Environment for Statistical Computing (R Foundation for Statistical Computing).

RESULTS

A quantitative method for NCS assessment was developed returning percentage of EECs with NCSs per endometrial biopsy (Fig. 1A). Agreement between two independent observers on 25 samples for percentage of EECs with NCSs was excellent (r^2 = 0.99; linear regression), as well as for the total count of NCSs (ICC = 0.96; 95% confidence interval [CI] 0.93 - 1.00) and EECs (ICC = 0.97; 95% CI 0.96 - 0.98). The high degree of agreement justifies the use of a single observer with our new NCS quantification method. Additionally, based on the percentage of EECs with NCSs of five different paraffin

sections from the same sample (22.8 ± 1.3%), the intrasample variability of the assay was low (coefficient of variation 0.06).

Overall, 42 hysterectomy specimens were enrolled, 30 of which were declared as secretory-phase endometria by the clinical pathologist. Classic histologic dating was successfully performed on 29 of the 30 secretory-phase specimens; one specimen had insufficient tissue for definitive dating. Ten uteri were given histologic dates of CD 18–24. Of these, nine had sufficient tissue for further analysis and eight exhibited >5% EECs with NCSs in at least one of the six sampled regions of the endometrial cavity, as did the lone undated specimen, for a total of nine uteri (Table 2).

NCSs appeared uniformly in the upper uterine cavity among these nine uteri (Fig. 1B). Collectively, the upper five regions (excluding the LUS) demonstrated a median number of EECs with NCSs of 16.9% (IQR 12.7–23.4), whereas the number of EECs with NCSs in the LUS of 6.1% (IQR 3.0–9.9) was significantly lower ($P=.008$; Wilcoxon signed ranks test; Fig. 1B). Analysis of the endometrial layers in all six regions of one uterus (Fig. 1B, yellow dots; Table 2, no. 9), demonstrated that NCSs were predominant in the stratum functionalis, the luminal (38 ± 9%) and middle layers (46 ± 9%), as compared to the basal layer (17 ± 6%; $P=.004$; one-way ANOVA; Fig. 1C). In contrast, the number of glands was evenly distributed among the three layers (luminal: 27 ± 9%; middle: 36 ± 4%; basal: 37 ± 8%; $P=.132$; Fig. 1C).

DISCUSSION

We demonstrate that one of the histologic hallmarks of secretory transformation and a marker for the midluteal endometrium, the NCS, is equally present in fundal, cornual (left and right), and midcavity (anterior and posterior) uterine sections. Clearly, there is no predisposition for the cornua. These findings are consistent with a morphometric study wherein 11 of 12 indices among endometrial biopsies taken from three different regions failed to show differences (25) and which forms the basis for the use of a single, presumably fundal, endometrial biopsy specimen in clinical practice. Nonetheless, our results are surprising given the specificity of the NCS for the midluteal phase (6, 7) and the decades of ultrastructural data setting the NCS apart from other histologic criteria and suggesting a role for it in endometrial receptivity. Overall, our data reinforce the findings that secretory transformation is not region-specific and lags only in the LUS and suggest that endometrial receptivity is achieved in a uniform fashion.

Human embryo implantation is subject to strict temporal specificity, known as the implantation window, which is limited to CD 20–24 based on results from anatomic dissection (20), an ovum donor/recipient model (26), and epidemiologic surveillance with the use of urinary hormonal metabolites (27). The question as to whether there is spatial specificity, or predisposition for implantation in (a) particular region(s) of the endometrial cavity, has been addressed by only a few studies (Table 1) and remains unresolved. In fact, despite the remarkable changes that the endometrium undergoes each month, there is little information about local fluctuations. Additionally, literature does exist regarding the optimal placement of the catheter tip during the embryo transfers (28–31). Those studies, however, merely establish the importance of avoiding fundal contact and the deleterious uterine contractility that ensues and, perhaps, the utility of an embryo transfer directed toward the lower or middle portions of the endometrial cavity rather than toward the fundus. They are not definitive regarding the specific location frequencies of implantation. On the other hand, the studies in Table 1 collectively suggest that the cornual region might prove most favorable for blastocyst implantation. Indeed, a reported criterion for ultrasonographically differentiating a gestational sac from a pseudogestational sac is the eccentric (lateral) location of the former versus the central (midline) presentation of the latter (32). Anatomic rationale attributes the lateral predisposition of blastocyst implantation to the superior vascularization of the lateral endometrium and cornua due to abundant anastomoses of the ascending uterine and adnexal vasculature (32, 33). Also,

TABLE 2

Patient information and nucleolar channel system (NCS) prevalence by uterine region.

	Patient									
	1	**2**	**3**	**4**	**5**	**6**	**7**	**8**	**9**	**Mean ± SD**
Age, y	42	41	47	42	42	45	43	44	46	43.6 ± 2.1
Cycle day (LMP)	20	22	NA	19	17	23	24	19	19	20.4 ± 2.4
Cycle day (Noyes)	20	23	NA	18	18	19	19	20	19	19.5 ± 1.6
Parous	+	−	+	+	+	+	+	+	+	8/9
Intramural Fibroids	+	+	+	+	+	+	+	+	+	9/9
Submucosal Fibroids	+	+	+	−	−	−	−	−	+	4/9
Percentage of EECs with NCSs										**Median (IQR)**
Fundus	19.6	14.6	5.4	24.6	10.3	18.1	32.8	11.2	10.9	14.6 (10.6–22.1)
Left cornu	15.4	7.8	20.9	38.2	22.2	15.8	41.9	18.8	11.7	18.8 (13.6–30.2)
Right cornu	27.7	12.1	14.2	21.3	21.1	16.9	50.0	11.7	14.7	16.9 (13.2–24.5)
Anterior body	18.2	14.3	14.0	26.6	11.5	30.3	48.7	12.6	13.2	14.3 (12.9–28.5)
Posterior body	17.2	15.4	17.9	35.6	22.2	5.4	52.7	12.7	12.9	17.2 (12.8–28.9)
Lower uterine segment	11.3	NA	0.5	6.7	5.4	2.3	10.8	4.9	7.2	6.1 (3.0–9.9)

Note: EEC = endometrial epithelial cell; IQR = interquartile range; LMP = last menstrual period.

Szmyga. NCSs appear throughout the endometrium. Fertil Steril 2013.

the free-floating blastocyst might prefer the ipsilateral cornu owing either to having encountered it first upon its egress from the fallopian tube or to as yet uncharacterized localized signaling.

Regardless, NCS prevalence is uniform in the upper endometrial cavity, and undisturbed by such lateral predisposition. The significantly lower prevalence of the NCS in the LUS is consistent with earlier studies. Noyes et al. (21) already noted the lag in secretory transformation of the LUS—"Tissue from the fundus of the uterus gives more reliable information than that from the lower uterine segment"—and this finding has been endorsed in the subsequent literature (34). This defect in secretory transformation seems at least partially responsible for the low likelihood of lower segment implantation in unscarred uteri (placenta previa).

In addition to a preference for the upper endometrial cavity, NCSs show a preference for the endometrial luminal and middle layers in all uterine regions compared with the basal layer (Fig. 1C). This is in contrast to the even distribution of glands. NCS prevalence in the luminal and middle layers highlights a hitherto unappreciated polarity of the endometrium and further underlines the physiologic significance of NCSs, because those are the functionally important layers supporting implantation and being renewed during each cycle.

Of interest, the mere presence of intramural fibroids does not affect NCS appearance and, by extension, does not impede secretory transformation. The presence of intramural fibroids among our study specimens was ubiquitous (38/42 [90%] overall and 10/10 [100%] among the midluteal specimens) and is not surprising given that we specifically targeted benign hysterectomy specimens among ovulatory women under the age of 50. The fact that the nine specimens with >5% EECs with NCSs in at least one region demonstrate >5% EECs with NCSs in every region that was sampled (Fig. 1; Table 2) gives us confidence that intramural fibroids do not impede secretory transformation and that this assertion is not vulnerable to type II error.

In summary, we used the region-specific appearance pattern of NCSs in the endometrial cavity to elucidate the question of regional predisposition for secretory transformation. Our finding that NCS presence is uniform throughout the upper endometrial cavity suggests symmetric transformation of the secretory-phase endometrium in the upper cavity, a process that appears to be impervious to the mere presence of intramural fibroids.

Acknowledgments: The authors thank Nanette Santoro (University of Colorado, Denver, Colorado) for her support of their work and for critical comments on the manuscript. They acknowledge the assistance of the Gynecology Service attending physicians and house staff at Montefiore Medical Center in enrolling hysterectomy specimens for this study. The authors are grateful to the Surgical Pathology staff at Montefiore Medical Center, Weiler Division (Charles Fernandez, Duhane McGregor, and Lin Zhang) for their assistance in obtaining the endometrial tissue sections. Statistical support was provided by the Einstein-Montefiore Institute for Clinical and Translational Research. All imaging was performed at the Analytical Imaging Facility and all slides prepared by the Histotechnology and Comparative Pathology Facility of the Albert Einstein College of Medicine.

REFERENCES

1. Cornillie FJ, Lauweryns JM, Brosens IA. Normal human endometrium. An ultrastructural survey. Gynecol Obstet Invest 1985;20:113–29.
2. Dubrauszky V, Pohlmann G. Strukturveränderungen am Nukleolus von Korpusendometriumzellen während der Sekretionsphase. Naturwissenschaften 1960;47:523–4.
3. Terzakis JA. The nucleolar channel system of human endometrium. J Cell Biol 1965;27:293–304.
4. Spornitz UM. The functional morphology of the human endometrium and decidua. Adv Anat Embryol Cell Biol 1992;124:1–99.
5. Clyman MJ. A new structure observed in the nucleolus of the human endometrial epithelial cell. Am J Obstet Gynecol 1963;86:430–2.
6. Guffanti E, Kittur N, Brodt ZN, Polotsky AJ, Kuokkanen SM, Heller DS, et al. Nuclear pore complex proteins mark the implantation window in human endometrium. J Cell Sci 2008;121:2037–45.
7. Rybak EA, Szmyga MJ, Zapantis G, Rausch M, Beshay VE, Polotsky AJ, et al. The nucleolar channel system reliably marks the midluteal endometrium regardless of fertility status: a fresh look at an old organelle. Fertil Steril 2011;95:1385–9.e1.
8. Dockery P, Pritchard K, Taylor A, Li TC, Warren MA, Cooke ID. The fine structure of the human endometrial glandular epithelium in cases of unexplained infertility: a morphometric study. Hum Reprod 1993;8:667–73.
9. Dockery P, Pritchard K, Warren MA, Li TC, Cooke ID. Changes in nuclear morphology in the human endometrial glandular epithelium in women with unexplained infertility. Hum Reprod 1996;11:2251–6.
10. Pryse-Davies J, Ryder TA, MacKenzie ML. In vivo production of the nucleolar channel system in post menopausal endometrium. Cell Tissue Res 1979; 203:493–8.
11. Demir R, Kayisli UA, Celik-Ozenci C, Korgun ET, Demir-Weusten AY, Arici A. Structural differentiation of human uterine luminal and glandular epithelium during early pregnancy: an ultrastructural and immunohistochemical study. Placenta 2002;23:672–84.
12. Kohorn EI, Rice SI, Gordon MM. In vitro production of nucleolar channel system by progesterone in human endometrium. Nature 1970;228:671–2.
13. Kohorn EI, Rice SI, Hemperly SS, Gordon MM. The relation of the structure of progestational steroids to nucleolar differentiation in human endometrium. J Clin Endocrinol 1972;34:257–64.
14. Roberts DK, Horbelt DV, Powell LC. The ultrastructural response of human endometrium to medroxyprogesterone acetate. Am J Obstet Gynecol 1975;123:811–8.
15. Dockery P, Ismail RM, Li TC, Warren MA, Cooke ID. The effect of a single dose of mifepristone (RU486) on the fine structure of the human endometrium during the early luteal phase. Hum Reprod 1997;12:1778–84.
16. More IA, McSeveney D. The three dimensional structure of the nucleolar channel system in the endometrial glandular cell: serial sectioning and high voltage electron microscopic studies. J Anat 1980;130:673–82.
17. Cavagna M, Contart P, Petersen CG, Mauri AL, Martins AMC, Baruffi RLR, et al. Implantation sites after embryo transfer into the central area of the uterine cavity. Reprod Biomed Online 2006;13:541–6.
18. Kawakami Y, Andoh K, Mizunuma H, Yamada K, Itoh M, Ibuki Y. Assessment of the implantation site by transvaginal ultrasonography. Fertil Steril 1993;59:1003–6.
19. Minami S, Ishihara K, Araki T. Determination of blastocyst implantation site in spontaneous pregnancies using three-dimensional transvaginal ultrasound. J Nippon Med Sch 2003;70:250–4.
20. Hertig A, Rock J, Adams EC. A description of 34 human ova within the first 17 days of development. Am J Anat 1956;98:435–93.
21. Noyes RW, Hertig A, Rock J. Dating the endometrial biopsy. Fertil Steril 1950; 1:3–25.
22. Murray M, Meyer W, Zaino R, Lessey B, Novotny D, Ireland K, et al. A critical analysis of the accuracy, reproducibility, and clinical utility of histologic endometrial dating in fertile women. Fertil Steril 2004;81:1333–43.

23. Werner M, Chott A, Fabiano A, Battifora H. Effect of formalin tissue fixation and processing on immunohistochemistry. Am J Surg Pathol 2000;24:1016–9.
24. Houghton JP, Roddy SS, Carroll SS, McCluggage WG. A simple method for the prevention of endometrial autolysis in hysterectomy specimens. J Clin Pathol 2004;57:332–3.
25. Johannisson EE, Parker RAR, Landgren BMB, Diczfalusy EE. Morphometric analysis of the human endometrium in relation to peripheral hormone levels. Fertil Steril 1982;38:564–71.
26. Bergh PA, Navot D. The impact of embryonic development and endometrial maturity on the timing of implantation. Fertil Steril 1992;58:537–42.
27. Wilcox AJ, Baird DD, Weinberg CR. Time of implantation of the conceptus and loss of pregnancy. N Engl J Med 1999;340:1796–9.
28. Waterstone J, Curson R, Parsons J. Embryo transfer to low uterine cavity. Lancet 1991;337:1413.
29. Coroleu B, Barri PN, Carreras O, Martínez F, Parriego M, Hereter L, et al. The influence of the depth of embryo replacement into the uterine cavity on implantation rates after IVF: a controlled, ultrasound-guided study. Hum Reprod 2002;17:341–6.
30. Frankfurter D, Trimarchi JB, Silva CP, Keefe DL. Middle to lower uterine segment embryo transfer improves implantation and pregnancy rates compared with fundal embryo transfer. Fertil Steril 2004;81:1273–7.
31. Pope CS, Cook EKD, Arny M, Novak A, Grow DR. Influence of embryo transfer depth on in vitro fertilization and embryo transfer outcomes. Fertil Steril 2004;81:51–8.
32. Abramovici H, Auslender R, Lewin A, Faktor JH. Gestational-pseudogestational sac: a new ultrasonic criterion for differential diagnosis. Am J Obstet Gynecol 1983;145:377–9.
33. Itskovitz J, Lindenbaum ES, Brandes JM. Arterial anastomosis in the pregnant human uterus. Obstet Gynecol 1980;55:67–71.
34. Robertson W. A reappraisal of the endometrium in infertility. Clin Obstet Gynaecol 1984;11:209–26.